Clément BARAILLE

Biomed
2022-2023

CRMBM, UMR 7339, CRNS, Aix-Marseille Université
27 Bd Jean Moulin, 13385 Marseille

Spinal cord T1 relaxation and use of Z-score maps to identify pathological tissues

from 15/05/2023 to 21/07/2023

Under the supervision of:

- **Internship supervisor: Virginie CALLOT, virginie.callot@univ-amu.fr**
- **School supervisor: Franz BRUCKERT, franz.bruckert@grenoble-inp.fr**

Confidentiality : NO

Ecole nationale
supérieure de physique,
électronique, matériaux

Phelma
Bât. Grenoble INP - Minatec
3 Parvis Louis Néel - CS 50257
F-38016 Grenoble Cedex 01

Tél +33 (0)4 56 52 91 00
Fax +33 (0)4 56 52 91 03

http://phelma.grenoble-inp.fr

Acknowledgments

First and foremost, I would like to express my sincerest gratitude to my lab supervisor, Virginie Callot. She spent a lot of time to bring me the medical background required to complete my missions and allowed me to discover the sophisticated field of the biomedical research. She made herself very available and always helped me.

I would also like to thank Dr. Kaissar Farah, with whom I worked during my second mission. He made me understand what was at stake during this project, and took the time to explain the results he had already obtained.

Finally, I would like to thank my co-workers with whom I shared the office for maintaining a nice atmosphere during my whole internship.

This internship was supported thanks to funding from France Life Imaging.

Contents

Glossary

- MR : Magnetic Resonance
- MRI : Magnetic Resonance Imaging
- MRS : Magnetic Resonance Spectroscopy
- NMR : Nuclear Magnetic Resonance
- CNS : Central Nervous System
- SC : Spinal Cord
- WM : White Matter
- (ai)GM : (anterior + interior) Gray Matter
- ROI : Region Of Interest
- CST : Corticospinal Tract
- PST : Posterior Sensory Tract
- B_0 : Static magnetic field
- B_1 : Magnetic field applied to break the equilibrium of magnetization
- T_1 : Time which characterizes the longitudinal relaxation of magnetization after a perturbation
- T_2 : Time which characterizes the transverse relaxation of magnetization after a perturbation
- PAM50 : Template in which are registered the acquired data
- Atlas / Mask : Tool that helps to extract metrics in a specific area
- STD : Standard Deviation
- HC : Healthy Controls
- ALS : Amyotrophic Lateral Sclerosis
- DCM : Degenerative Cervical Myelopathy

List of f igures

List of Tables

1 Overview of the laboratory

The Centre de Résonance Magnétique Biologique et Médicale (CRMBM) and the Centre d'Exploration Métabolique par Résonance Magnétique (CEMEREM) are research units specialized in Magnetic Resonance (MR) techniques, respectively for animals and humans. Both located at the medical campus of La Timone (Marseille), they form the UMR 7339 (Unité Mixte de Recherche), managed by the CNRS (INSIS and INSB) and Aix-Marseille University.

At CEMEREM, researchers conduct a wide range of studies and investigations using advanced Magnetic Resonance Imaging (MRI) and Magnetic Resonance Spectroscopy (MRS) techniques. The laboratory is equipped with state-of-the-art facilities, especially with a 7 Tesla MRI device allowing high resolution imaging. Thus, researches on various aspects of human physiology, neuroscience, neurodegenerative diseases, cardiovascular disorders, and more can be carried out. The center collaborates with clinical teams and scientists from different disciplines to explore and understand the underlying mechanisms of various diseases and develop new diagnostic and therapeutic approaches.

The laboratory is divided into three research teams, respectively working on the Cardiovascular System, the Central Nervous System and the Musculoskeletal System.

Figure 1: Organizational chart of CRMBM-CEMEREM

During this internship, I had the opportunity to join the Central Nervous System (CNS) team, alongside Virginie CALLOT (Research Director, CNRS) who is the principal investigator of the Spinal Cord Imaging in the laboratory (https://crmbm.univ-amu.fr/topic/spinal-cord-imaging/). The Spinal Cord MRI research group has a primary goal of improving the non-invasive understanding of spinal cord impairments and contributing to the description of spinal cord pathophysiological mechanisms, through the development of quantitative and multi-parametric MRI techniques.

Leveraging a unique platform that encompasses small animal MR facilities, clinical research scanners, and ultra-high field systems, the Spinal Cord MR Imaging axis conducts comprehensive research across a broad spectrum. This includes studies ranging from experimental models to patient explorations, as well as encompassing dedicated MR methodological advancements and specialized post-processing tools. The group collaborates closely with academic and clinical partners in order to facilitate their research objectives.

2 Introduction

The following paragraphs briefly present some key-concepts for this internship : the spinal cord, the MR signal and the normalization space (template).

2.1 The Central Nervous System (CNS)

The central nervous system is a complex network of structures that includes the brain and spinal cord, serving as the primary control and processing center of the entire nervous system [1].

The brain, which is located within the skull, is responsible for a wide range of functions, including cognition, consciousness, memory, emotions, sensory processing, motor control, and coordination of bodily systems. It is divided into different regions, each with specific roles and interconnected through neural pathways.

The spinal cord, linked to the brain by the brainstem, is a long cylindrical bundle of nerve fibers that extends from the base of the brain down through the spinal column. It acts as a pathway for communication between the brain and the peripheral nervous system, which includes the nerves that branch out from the spinal cord to the rest of the body. The spinal cord relays sensory information from the body to the brain and transmits motor commands from the brain to the muscles and organs.

Both the brain and the spinal cord are composed of white matter and gray matter, essential for the proper functioning of the CNS. Gray matter contains cell bodies and is involved in information processing, while white matter consists of myelinated nerve fibers that facilitate communication between different areas of the CNS.

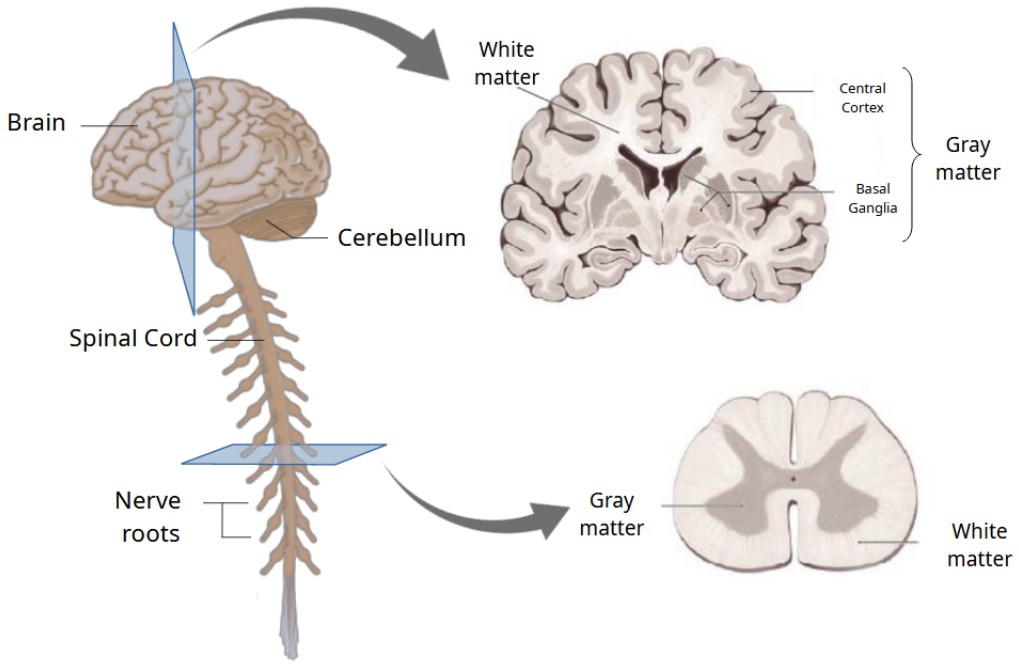

Figure 2: Simplified representation of the CNS

For a better understanding of the following work, it is necessary to know the basics of spinal cord composition. As mentioned previously, it is separated into white and gray matters, which also are divided into regions of interest (ROI), each corresponding to a precise function. The main

specific areas studied during my internship were :

- The corticospinal tract (CST) [2][3], originated in the motor cortex of the brain, which extends through the brainstem and descends into the spinal cord. Its fibers synapse with some motor neurons of the gray matter and play a crucial role in the voluntary control of skeletal muscles, especially in distal ends.
- The posterior sensory tract (PST)[3], divided into two specific tracts, the gracile fasciculus and the cuneate fasciculus which are respectively responsible information carrying in the lower and upper parts of the body. Together, they transmit sensory information related to fine touch, vibration, and proprioception from the body to the brain.

Actually, the Gray Matter is divided into two sections: the anterior + interior Gray Matter (aiGM) and the dorsal Gray Matter, which is a smaller structure. For the sake of accuracy in our upcoming study, we will focus on aiGM because of the spatial resolution of 3T MRI which could involve partial volume effect (cf. paragraph 3.3.2).

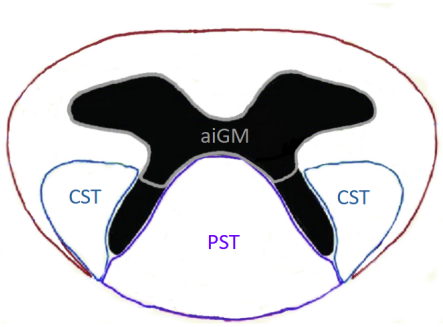

Figure 3: Location of the different ROIs in the spinal cord

Some pathologies affect these structures, such Multiple Sclerosis, with demyelination of WM, and ALS, with strong involvement of aiGM. Therefore, MRI plays a key role in the diagnosis of spinal cord pathologies when a neurological deficit is suspected.

2.2 Nuclear Magnetic Resonance and Magnetic Resonance Imaging principles

In matter, each nucleus has an intrinsic angular momentum called the spin, which leads to the existence of magnetic moments. In presence of a static magnetic field B_0, nuclear moments precess at a specific frequency, called the resonance frequency, also known as the Larmor frequency, which is proportional to B_0. Individually, these precessions cannot be detected, but together, they create a magnetization vector, which is collinear to the static field at equilibrium. However, its magnitude is negligible compared to B_0 and thus cannot be measured. Applying a radio-frequency pulse - a magnetic field B_1 at ω_e - destroys this equilibrium. At the end of this perturbation, the magnetization has rotated, and return to its original position. It is possible to characterize this phenomenon vectorially, with a longitudinal and a transverse relaxations. Both of them have an exponential shape, respectively increasing and decreasing. Finally, time constants, which depend on the tissue nature, are introduced to quantize these evolutions: T_1 characterizes the longitudinal magnetization, whereas T_2 is linked to the transverse one [4].

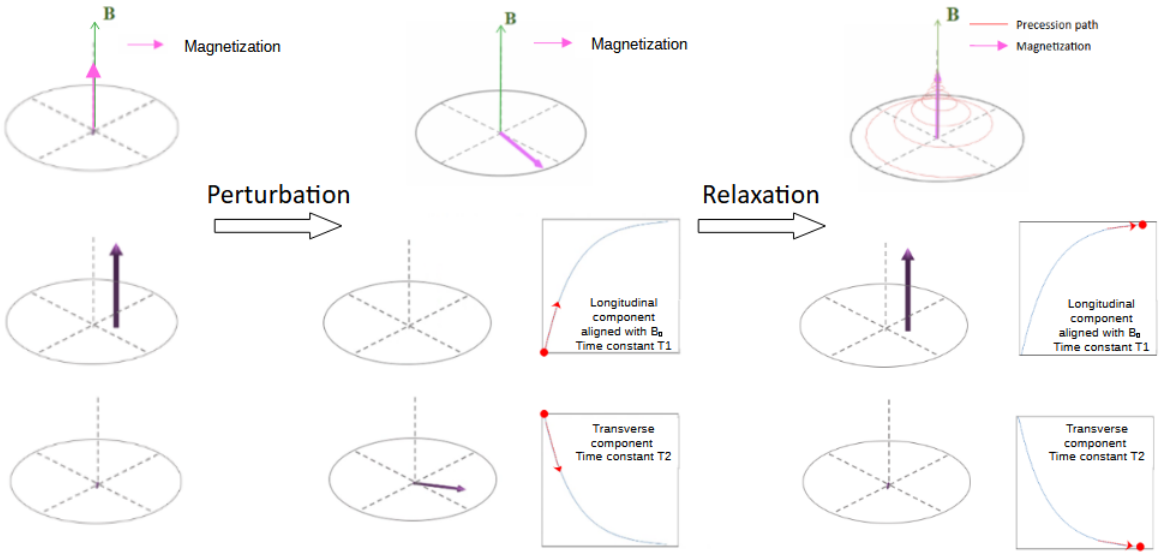

Figure 4: Evolution of magnetization after a perturbation

These relaxation times depend on the chemical compositions of tissues and are part of a RMN signal, which is acquired by antennas that allow focusing specific part of the body.

At this moment of the process the signal does not contain any spacial information that could allow the reconstitution of an image. However, if gradient fields are applied during the acquisition of the signal, each spatial location then acquires a specific frequency (signal encoding) [5]. Then, thanks to numerical processing (double Fourier Transformations), it is possible to reconstruct an intelligible image. Playing on parameters of the acquisition sequence (such as repetition time, echo time, inversion time) allow to obtain different contrasts in the image and differentiate tissues.
In clinical routine, qualitative images, weighted with different contrasts, are usually sufficient for diagnosis purpose, however quantitative methods may be required for a more objective assessments, prognosis or therapeutical evaluation.
In CEMEREM, researchers thus focus their researches on the development of quantitative MRI [6], such as diffusion MRI, perfusion MRI, magnetization transfer MRI or relaxometry (as used in this internship). Indeed, these relaxation times contain supplementary information on tissue physiology, allowing to detect anomalies and thus potentially guide clinical decisions.

2.3 Pre-processing of acquired data

When dealing with quantitative images, in order to facilitate subsequent analysis in specific regions of interest, a pre-processing of the images can be performed. In the case of my work, images needed to be registered in the PAM50 template [7]. The PAM50 is a normalisation space constructed by averaging spinal cord and brainstem MRI data of 50 healthy subjects, for 3 different contrasts (T_1w, T_2w and T_2*w). This template is associated to probabilistic atlases of different tracts in spinal cord [9] which provide the probability of a voxel (3D pixel) to belong to a specific region of interest.

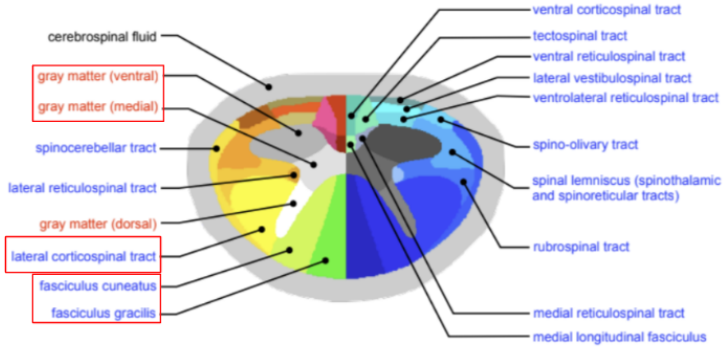

(a) Division of the spinal cord into 36 atlases

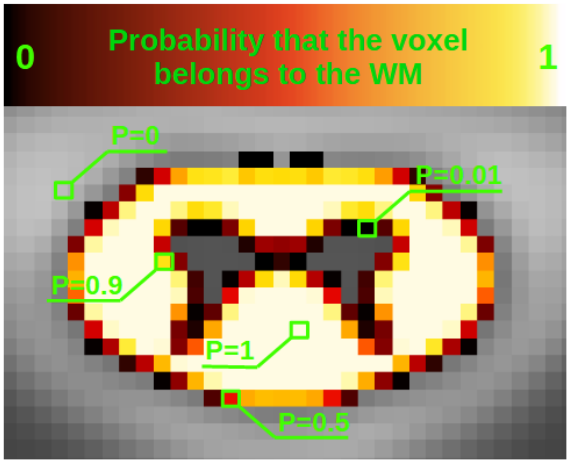

(b) Example of use of WM atlas

Figure 5: Explanation of atlases concept

These atlases avoid manual segmentation, which can be time consuming, and consequently improve reproducibility.

In order to coregister acquired data into the PAM50 space, the Spinal Cord Toolbox (a software dedicated to the processing and analysis of spinal cord MRI data) is used as a preliminary step. Thereby, the spinal cord is first automatically segmented. Then, the spinal cord image, which is originally curved, is straightened and resized to fit the template. Landmarks (vertebral labelling) can be used to help the non linear coregistration from the straightened cord to the template. Registration and template based analysis can be realized for both healthy and pathological data.

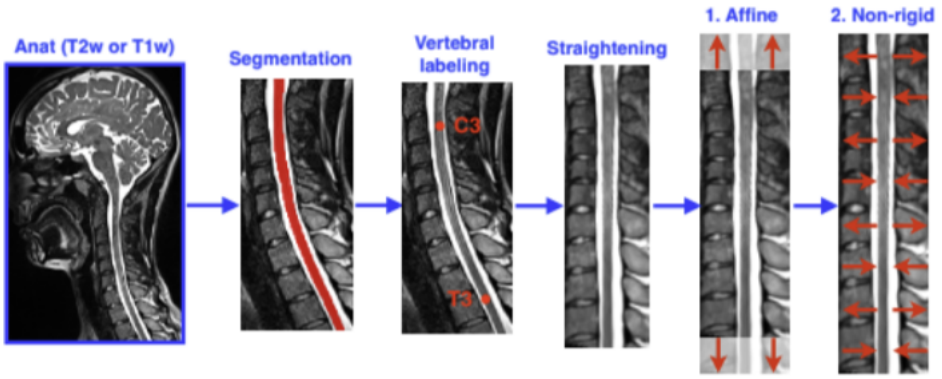

Figure 6: Illustration of the different steps allowing to register new data into the PAM50 template space

2.4 Spinal Cord impairments and neurodegenerative diseases

Spinal cord impairments and neurodegenerative diseases are two distinct yet interconnected categories of neurological conditions that can significantly impact quality of life.
Spinal cord impairments typically arise from traumatic injuries, infections, tumors, or congenital abnormalities affecting the spinal cord's structure and function. As explained earlier, these impairments can lead to varying degrees of motor, sensory, and autonomic dysfunction, often resulting in paralysis or loss of sensation below the level of injury.
On the other hand, neurodegenerative diseases encompass a range of chronic and progressive conditions, such as Alzheimer's disease, Parkinson's disease, and Amyotrophic Lateral Sclerosis (ALS), or Multiple Sclerosis where there is a gradual deterioration of neurons and brain functions over time. These diseases manifest with a wide array of symptoms, including memory loss, movement disorders, cognitive decline, and speech difficulties.
Despite their diverse origins, both spinal cord impairments and neurodegenerative diseases present substantial challenges, emphasizing the critical need for ongoing research, medical interventions, and supportive care to improve the lives of those affected.
From the research point of view in the lab, this translates into the development of more specific and robust MR methods that can overcome challenges related to the cord (such as small size, physiological motions, susceptibility artifacts), but also by the developments of specific tools that may allow to facilitate the investigation and the identification of specific and relevant biomarkers. The implementation of such tools was part of my internship. The following paragraph briefly details my objectives and missions.

2.5 Main objectives of my internship

In my internship, I had to deal with MR data previously acquired in both healthy and pathological subjects using an MP2RAGE sequence. The MP2RAGE sequence was initially proposed for brain exploration [10], and it has been optimized in the lab for cord investigation [11], where it has been demonstrated as a promising tool [12]. The MP2RAGE sequence provides quantitative T_1 measurements that can be used to describe the soft tissues and their substructures [13], as well as their impairments. In order to facilitate such pathological explorations, one of my first mission was to develop a program that allows investigating the potentialities offered by z-score maps. This technique was then applied to 2 cohorts of patients, one suffering from Amyotrophic Lateral Sclerosis (ALS), the other one from Degenerative Cervical Myelopathy (DCM). Finally, I also had to work on a program that could help users to properly use the MP2RAGE sequence, and evaluate its robustness with regard to radiofrequency inhomogeneity (detailed later) and protocol parameters.

3 Main achievements during my internship

The concept of z-score is first briefly summarized in the next paragraph. Then, the core of my work and its implementation are presented.

3.1 Data analyses using the Z-score

In the case of my work, all datasets were already coregistered in the PAM50 space. Each voxel of MRI data corresponds to a T_1 value (T_1q, in milliseconds). Inside the white and gray matters, a high value of T_1 can highlight the presence of abnormalities which can be further used for diagnosis, or to describe the tissue alteration. Thus, it may be interesting to investigate automatic detection of these abnormal or outlier values (as compared to values usually observed in normal situation). One simple mathematical approach could be the computation of Z-scores. [14] In statistics, the Z-score (or standard score) is a measure that indicates how many standard deviations an observation or data point is from the mean of a distribution. It is useful because it allows to compare values from different distributions or datasets (here healthy versus pathological for instance). By standardizing the data, one can determine how extreme or unusual a particular value is compared to the rest of the data.

The usual formula to compute the Z-score of a random variable X following a normal distribution (mean = μ and standard deviation = σ) is:

$$Z_{score}(X) = \frac{X-\mu}{\sigma}$$

Fortunately, the package fslmaths [15] allows to perform operations on MRI data:

- basics operations: it is possible to add, substract, multiply and divide one MRI dataset by another.
- fslmaths -Tmean: this function takes several MRI files as entries and generate an average map. For instance, the voxel of coordinates (x,y,z) of the generated file is the mean of the voxels (x,y,z) from all the entries.
- fslmaths -std: this function takes several MRI files as entries and generate a standard deviation (STD) map. For instance, the voxel of coordinates (x,y,z) of the generated file is the standard deviation of the voxels (x,y,z) from all the entries.

Thus, thanks to these functions, the Z-score map of a patient i can be computed using the following formula:

$$Z_{score}(i) = \frac{T_{1q}^{i} - \overline{T_{1q}^{AllHC}}}{\sigma[T_{1q}^{AllHC}]}$$

where T_{1q}^{i} corresponds to the T_1 map of a patient, $\overline{T_{1q}^{AllHC}}$ is the mean map generated from HC and $\sigma[T_{1q}^{AllHC}]$ is the standard deviation map generated from HC. It is possible to generate a whole Z-map for each patient, where a Z-score locally superior to 2 (or inferior to -2) should be characteristic of a particularly high or low T_1 value, potentially corresponding to lesions or tissue impairments in the SC.

Here are examples of Z-score calculations for both classical and MRI datasets.

Classical data

- Considering a random variable $X \sim \mathcal{N}(\mu, \sigma^2)$
- The mean of the distribution is μ
- The standard deviation of the distribution is σ
- A value of Z-score can be computed for each realisation of the random variable X, using the following formula :

$$Z_{score}(X) = \frac{X-\mu}{\sigma}$$

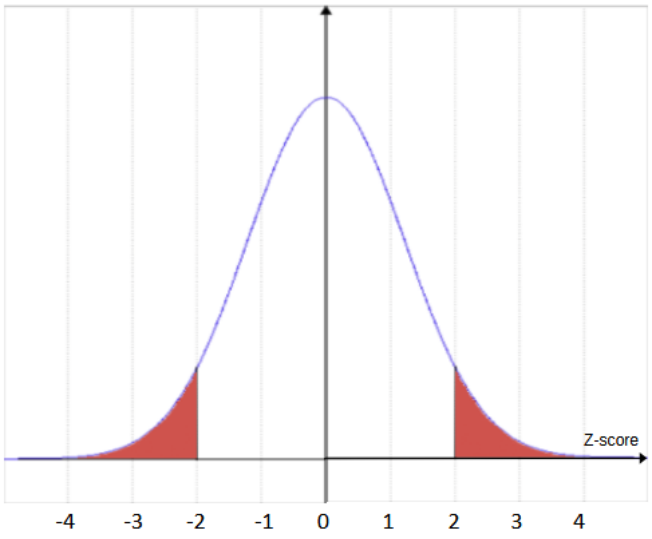

Figure 7: Probability density for normal distribution. Red areas correspond to Z-score higher than 2 (in absolute value).

MRI data

- Considering a cohort of N healthy controls and 1 pathological
- A mean file of the HC can be generated by averaging voxels of each HC
- A STD file of the HC can be generated by computing the standard deviation of each voxels from HC
- Each voxel will have a Z-score, computed using to the following formula :

$$Z_{score}(i) = \frac{T_{1q}^{i} - \overline{T_{1q}^{AllHC}}}{\sigma[T_{1q}^{AllHC}]}$$

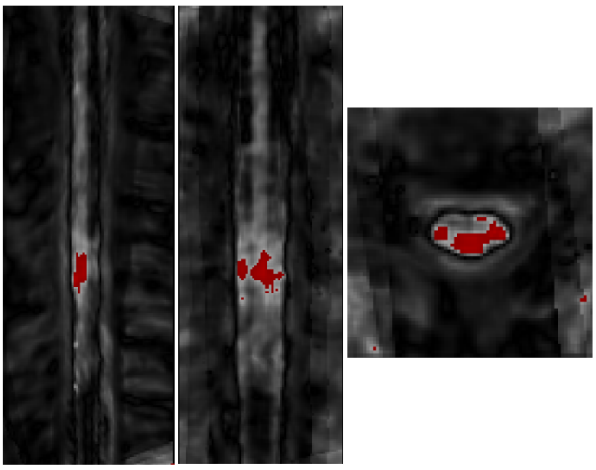

Figure 8: Z-map of the pathological example. Red areas correspond to regions of high Z-score, that could correspond to lesions.

3.2 Preliminary work

3.2.1 Preparation of databases

As explained previously, the Z-score computation relies on the comparison between pathological cases and healthy controls. Thus, it is important to choose wisely the HC database in order to optimize the Z-score computation.

First and foremost, the population that constitutes the dataset must be large enough in order to allow consistent comparisons. Usually, the dataset should count at least 30 samples [16].

Then, the MRI files on CEMEREM's servers came from two different MRI machines: Verio 3T and Vida 3T. However, after comparing acquisitions from both machines, a systematic bias has been highlighted: the T_1 measured in the spinal cord by the Vida machine were higher than those acquired by Verio (ΔT_{1mean}=29.8ms). This gap was not negligible, hence the necessity to split the whole HC database in two, and only compare Verio pathological subjects (respectively Vida pathological subjects) to Verio HC (respectively Vida HC) to gain in sensitivity (although splitting the database could decrease its statistical power).

Finally, it has been established that, in the spinal cord, T_1 values tend to decrease with age, until a maturation age around 50 years, and then increase [17]. It might not be relevant to compare a 30 years old patient to a HC cohort which median age is around 50.

Thus, the original HC database needed to be sorted by machine, and by age. To ease the establishment of databases appropriate to each patient, and determine which one would be the best for Z-score computation, the following programs have been implemented on Matlab:

- A program gathering all the datafiles from a same machine, compute their mean and their standard deviation. This is the **"static approach"**.
- A program gathering the datafiles from a same machine within an age decade. For instance, if the patient is 34 years old and acquired by Verio, it can compute the mean and std of datafiles from HC aged between 30 and 39 years from Verio machine. This is the **"decade approach"**.
- A program gathering the datafiles from a certain number of HC, acquired by a same machine, for which the median age match the patient's. For instance, for a 57 years old patient, acquired by Vida, it will create a database of N HC acquired by Vida, which median age is around 57, and then generate the mean and std file. This is the **"N-dynamic approach"**.

These three approaches will be compared to figure which one provides the best results, considering the initial database at disposal.

3.2.2 Mask preparation

Instead of evaluating the whole Z-map generated, it is better to focus on specific ROIs to extract useful metrics. This is the role of atlases, that can be used as masks, mentioned previously. In the case of my work, 5 different ROIs were studied: the whole SC, WM, aiGM, cst and pst. However, for what we intended, they could not directly be used as they were provided by the toolbox. They need to be processed.

First, probabilistic atlases were binarized: a voxel for which the probabilistic value is higher than 0.5 is set to 1, else it is set to 0. Then, to minimize the partial volume effect, which is a conflict of tissues within a same voxel, masks have been eroded. It ensures that the area where the metrics are evaluated does indeed belongs to the ROI. This is a rather conservative approach (probabilistic values could have been used instead), chosen to minimize the in-roi standard deviation and make the comparison between the different approaches easier.

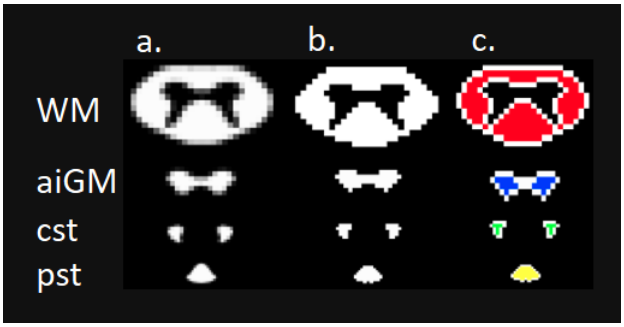

Figure 9: Processing of atlases. (a) Atlases provided by the SCT. (b) Atlases after binarization. (c) Atlases after erosion (coloured) compared to the binarized (white).

3.2.3 Quality assessment

The final step of this preliminary work was a quality assessment. I had to ensure that, among the MRI data I had at disposal, all of them were usable. Indeed, because of the overall process, some files could be lacking data, could contain artefacts or not be registered properly in the PAM50 template. Considering such outliers could jeopardize the Z-score results. In the end, each file has been cropped to a specific size to prevent missing slices, and two files, one from a HC and the other from a patient, have been discarded.

3.3 Analysis of Z-score for ALS patients

3.3.1 What is ALS ?

Amyotrophic lateral sclerosis (ALS), briefly mentionned in the introduction, and also known as "Maladie de Charcot" is a degenerative disease affecting motor neurons, located in the brain and spinal cord, responsible of voluntary muscle movements [18]. Causes of this pathology are not well-known yet: for 10% of the patients, the ALS is said to be "familial", when two cases occur within a family, and for the others, patients are called "sporadic", meaning that no clear pattern can be identified. The disease is progressive, which means symptoms worsen over time. As motor neurons degenerate and die, messages are no longer transmitted from the brain to the muscles, leading to impairment of the latters. This results in difficulties, or even impossibility, in walking, talking, swallowing and even breathing. This condition usually declares at a grown age and evolve into complete paralysis of the patients in the 3 to 5 following years[18], but few of them manage to live more than 10 years after the diagnosis. Because of the heterogeneity of the disease, it is complex to establish diagnosis or prognosis, even if abnormalities detection has been improved by brain and spinal cord MRI, and it remains important to identify some biomarkers.

3.3.2 Materials and methods

This study has been carried out from MRI data of 12 patients (9 men, 3 women; age, 55.6 $\pm$ 12.9 years; range, 33 - 75 years), diagnosed with ALS. They have been compared to a first HC cohort composed of 26 individuals (15 men, 11 women; age, 39.8 $\pm$ 15.7 years; range, 22 - 72 years), and a second age-centered HC cohort of 10 individuals (4 men, 6 women; age, 55.9 $\pm$ 10.5 years; range, 41 - 72 years).

MR acquisitions were performed using 3T MRI (MAGNETOM Verio; Siemens Healthcare, Erlangen, Germany).

3.3.3 Clinical assessment

To quantize the evolution of ALS, motor disabilities can be evaluated using the Revised ALS Functional Rating Scale (ALSFRS-R) [19]. It is a scoring over 48 points (normal value, 48; minimum, 0) that marks 12 physical functions going from writing to breathing over 4 points. Thus, patients with a high score in the 12 domains present better physical functions. Combined with the disease duration, the speed evolution of the condition can be computed thanks to another statistics: the disease progression rate (DPR). Included between 0 and 1, the higher is the DPR, the more serious is the evolution of the disease. Finally, the Spinal ALSFRS score (normal value, 36; minimum, 0) can be derived from the ALSFRS by focusing on functions relative to spinal cord.

	Median	Interquartile range	Min - Max
Disease duration (months)	16	[11.75 - 30]	[11 - 132]
Total ALSFRS-R (0–48)	44	[39.75 - 45.25]	[31 - 47]
Spinal ALSFRS-R subscore (0-36)	32	[28.75 - 33]	[21 - 36]
Disease progression rate	0.2	[0.1025 - 0.4375]	[0.03 - 0.82]

Table 1: Clinical features of the 12 patients with ALS included in this study

3.3.4 Results

Previous studies using T_1q MRI have already showed that the main difference between ALS patients and HC can be observed in the cst area [11]. In this study, T_1 mapping of the mean of the ALS cohort I had at disposal confirmed these results.

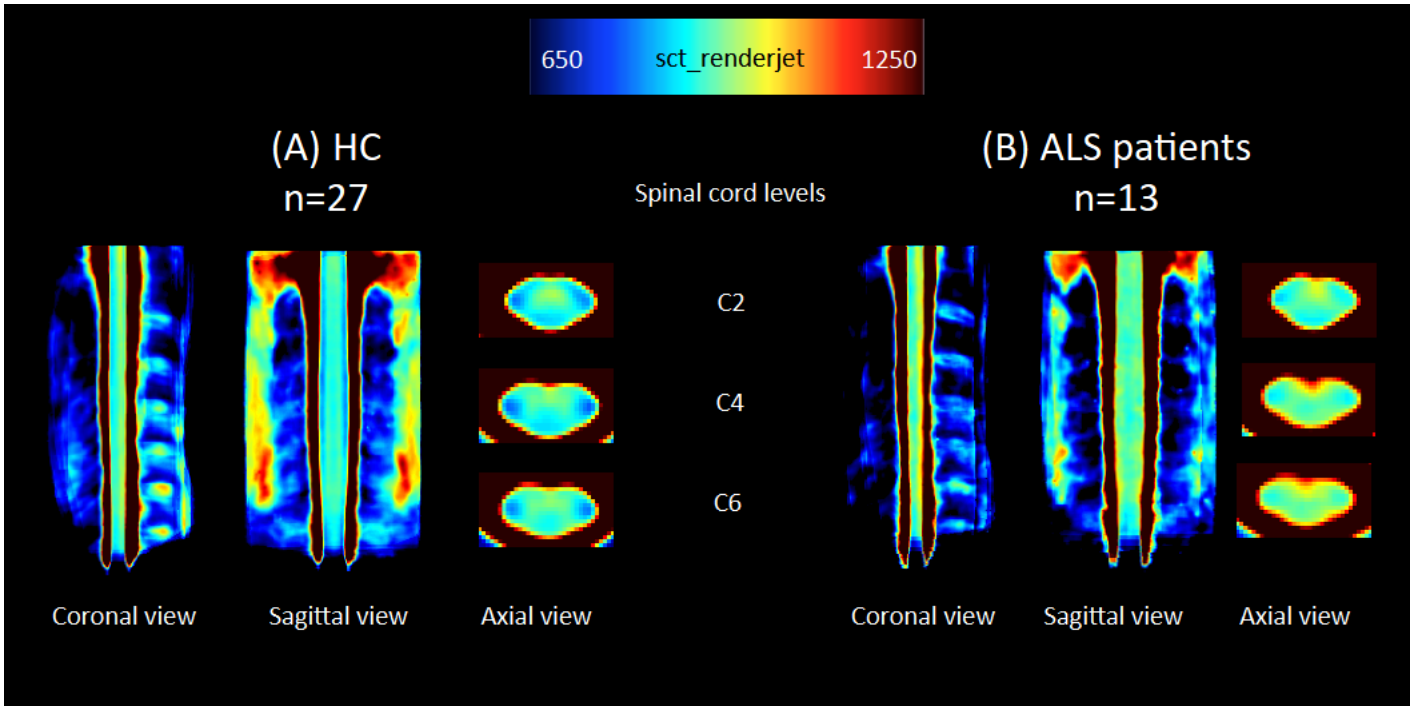

Figure 10: T_1 maps of HC (left) and ALS patients (right) in the PAM50 space. Higher T_1 can be observed in the corticospinal tracts of the patients, indicative of WM fiber degeneration consecutive to motoneuron death.

These results suggest that the Z-score for ALS patients should be higher in cst.

Comparing the “static”, “decade”, “10-dynamic” and “20-dynamic” approaches to compute the Z-scores of ALS patient, it turns out that **the “static” one was providing the best results, comparing the pathological cases to the gathering of every patients from a same machine**. Z-scores were the highest using the HC from the same decade and the same machine, but on the one hand, it could lead to false positives detection (Z-score ¿ 2 even without any lesion) and on the other hand, there were not enough samples from each decade to provide robust statistical results.
Z-scores have been computed in the whole SC, WM, aiGM, cst and pst ROIs for each individual patient, and then for the mean file of pathological cases. As expected, a mean Z-score higher than 2 has been measured in cst of upper cervicals, suggesting abnormalities.

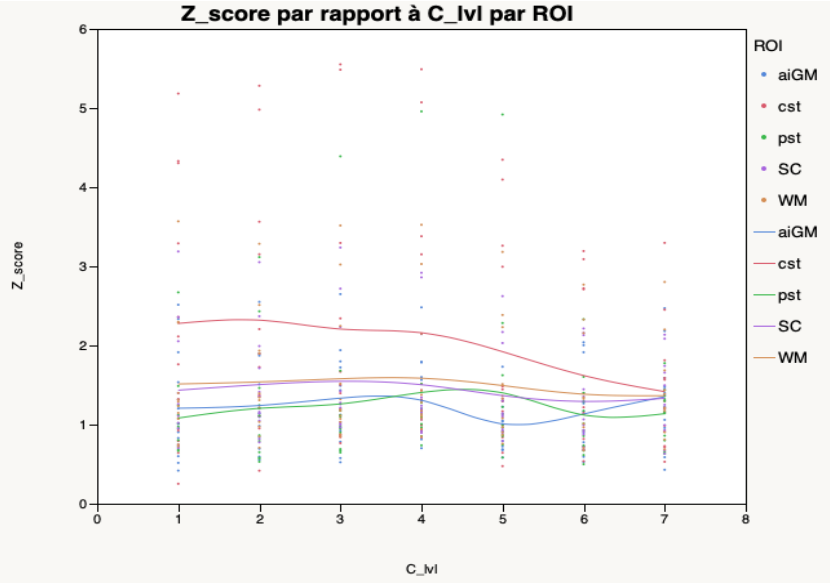

Figure 11: Mean Z-score of the 12 ALS patients in the different ROIs

Individually, only 4 of the 12 patients presented a Z-score higher than 2 for both lower and upper levels in cst. This threshold has also been exceeded in the whole SC and WM, but only for 3 patients.

Linear regressions have been computed for each scoring clinic with Z-score. Considering that a result is consistent if the p-value is lower than 5% [20] and the regression coefficient higher than 0.5, **only the disease duration seems to be correlated with Z-score, particularly in pst and WM.**

3.3.5 Discussion

In this work, Z-score has been used to facilitate cord tissue impairment detection in the spinal cord. However, this investigation is still in its embryonic stage and requires further researches. The use of a more appropriate database of HC should increase the accuracy of the process, especially by using a larger dataset age-centered on each patient. At this stage, it cannot be used as a tool which leads to clinical decisions, but rather as a complementary that can eventually confirm results.

3.4 Z-score for cervical myelopathy patients

3.4.1 What is cervical myelopathy ?

Cervical myelopathy is a medical condition occuring when there is compression or damage to the spinal cord, in the cervical region [21]. The most common cause of cervical myelopathy is degenerative changes in the cervical spine due to aging (degenerative cervical myelopathy, DCM). As people get older, the intervertebral discs between the vertebrae may degenerate, narrowing the spinal canal. This narrowing of the spinal canal can put pressure on the spinal cord, leading to compression and dysfunction of the nerves. Because of the wide range of symptoms, from simple numbness to incomplete paralysis, the cervical myelopathy is hard to diagnose. First, a medical treatment is provided and if symptoms remain, surgery is employed. On the one hand, damaged cervicals can be fixed one to the other whereas on the other hand it is possible to remove a portion of the vertebral bone in order to release pressure on the cord. These surgical procedures are respectively called arthrodesis and laminectomy [22]. Generally, the operation stops the progression of the pathology and may allow the regression of symptoms in some cases.

3.4.2 Materials and methods

This study has been carried out from MRI data of 17 patients (10 men, 7 women; age, 56.5 $\pm$ 11.9 years; range, 31 - 72 years), diagnosed with cervical myelopathy. For each of them, we got an acquisition at month zero (M0), before the surgery and a follow up three months (M3) after the surgical procedure. They have been compared to a HC cohort composed of 70 individuals (44 men, 26 women; age, 44.2 $\pm$ 15.5 years; range, 21 - 79 years). MR acquisitions were performed using 3T MRI Verio and Vida.

3.4.3 Clinical assessment

An objective measure scale of the gravity of cervical myelopathy is the mJOA score (Modified Japanese Orthopaedic Association). It is a scoring over 18 points (normal value, 18; minimum, 0) which evaluates motor dysfunctions of upper and lower extremities, sensations and sphyncter dysfunctions [23]. Evaluating the mJOA in time allows to verify that the health status of a patient does not worsen.

	Median	Interquartile range	Min - Max
mJOA at M0	14	[13 - 15]	[10 - 16]
mJOA at M3	15	[15 - 16]	[10 - 17]

Table 2: Clinical features of the 17 patients with cervical myelopathy included in this study

3.4.4 Results

First, it is possible to focus on a single pathological case to predict, or provide some expectations on, what should be observed overall. On this example, the patient suffers from a severe compression between cervical levels C4 and C5, and despite the surgery, tissue suffering (T_1 hypersignal) was still observable at M3.

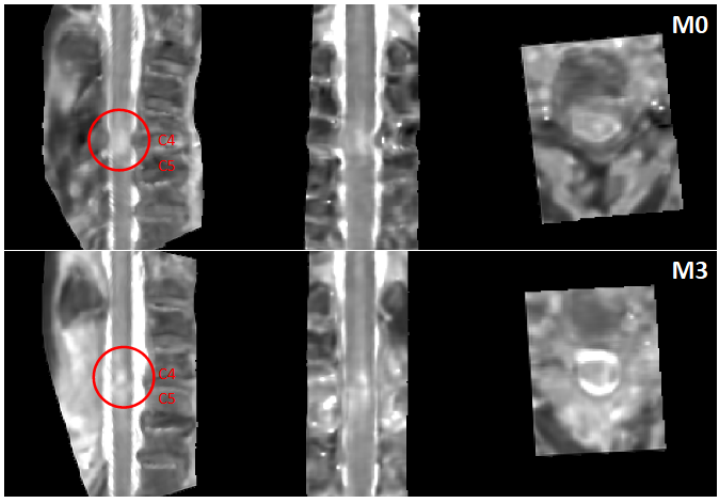

Figure 12: T_1 map of a cervical myelopathy patient at M0 (top) and M3 (bottom) in the PAM50 space. Compression area is circled in red.

For this patient, and every others suffering from myelopathy, the Z-score has been computed only in the whole spinal cord (rather than individual tracts).

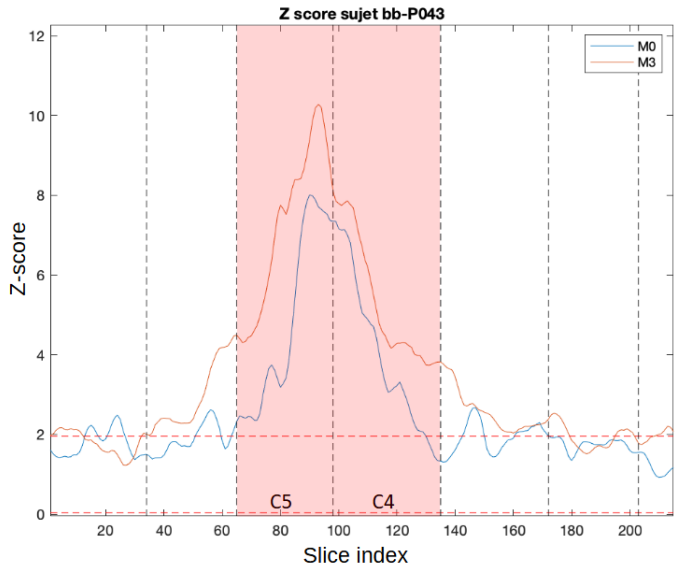

Figure 13: Evolution of Z-score along the cervical levels, at baseline (M0) and 3 months post surgery (M3) for a patient suffering from myelopathy

In this example, **the pathological region is clearly identified, between C4 and C5, and such a high Z-score can be interpreted as a tissue abnormality.** The Z-score is even higher 3 months post-surgery (M3), despite a stabilization of the mJOA patient (13 for both M0 and M3 exams).

These trends are also observable on the whole sample of myelopathy patients: the Z-score is above 2 on cervical levels C4-C5-C6, and globally increases in time, despite an improvement of the mJOA score.

To confirm, a linear regression has been computed between Z-score and mJOA. No consistent results (p-value $> 5\%$ and $r^2 < 0.5$) were obtained; these scores do not seem correlated.

3.4.5 Discussion

Compared to the previous study in ALS, the Z-score in DCM patients seems to be more indicative of the pathology. Moreover, it is localized in precise sites (interfaces between cervicals). However, it is important to keep in mind that the cohort of myelopathy cases used in this study was heterogeneous, with both single- and multi-stage cord compressions. Thus, results concerning the mean of the cohort have to be interpreted with care, since it would have been better to gather more patients, and divide the cohort according to the number of compressions.

3.5 Characterization of B_1 inhomogeneities

At the CEMEREM, the sequence used to acquire T_1 maps is called the Magnetization Prepared 2 Rapid Gradient Echo (MP2RAGE). It synthesizes an image from two acquisitions performed at two different inversion times. These two allow the calculation of a numerical UNI signal, included between -0.5 and 0.5, for which each value can be associated to a T_1 value thanks to a lookup table.

However, this technique is sensitive to radiofrequency inhomogeneities, also named B_1 inhomogeneities (ΔB_1) that could lead to biased and incorrect T_1 quantification and image reconstructions. Within the laboratory, these inhomogeneities are taken into account [24], and corrected, but it is not the case everywhere else.

3.5.1 The bias caused by B_1 inhomogeneities

Neglecting inhomogeneities, each value of UNI signal is theoretically associated to a single T_1 value. In reality, because radiofrequency inhomogeneities or B_1 inhomogeneities are present, the relationship between UNI and T_1 values is modified (cf. figure 14). According to the magnitude of inhomogeneities, a gap is observed between the T_1 that should theoretically correspond to a UNI value and the value measured with the actual one. It may result in a wrong colouring of T_1 map, and thus in a wrong representation of the observed region.

In this context, I build a short Matlab code that allows to quickly evaluate the T_1 bias as a function of B_1 inhomogeneity, depending on the MR protocol parameters used for the study (ie. inversion times, flip angles, ..).

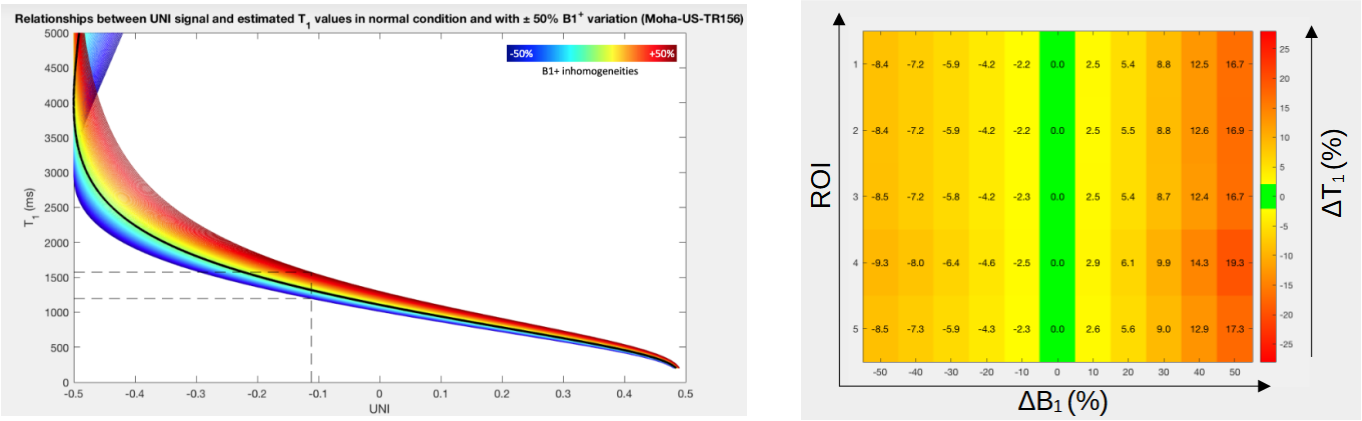

Figure 14: (a) Example of a lookup table connecting the UNI signal in a given voxel to the T_1values in that voxel for one of the protocol used in the lab (b) computation of the relative error on T_1 calculation (T_1 with appropriate B_1-correction versus T_1 without correction) for a given range of B_1 inhomogeneities (-50 to +50%), in 5 different ROIs in brain and cord, presenting with 5 different T_1.

To quantify the bias caused by B_1 inhomogeneities, we focused on five ROIs: SC cst (1), SC aiGM (2), brain occipital WM (3), brain occipital GM (4) and brain thalamus (5) , presenting with different T_1, respectively 902 ± [18;41;10] ms, 954 ± [35;32;10] ms, 790 ± [10;30;2] ms, 1318 ± [31;139;9] ms and 1053 ± [22;115;7] ms [25]. Each of these ROIs has been indexed to ease the reading of the table on figure 14.b. Different protocols of MP2RAGE have been tested, with various set of parameters and it turns out that the relative error measured on T_1 can reach 27.3% for $\Delta B_1 = 50\%$. Such bias would cause serious bias and confidence in the T_1 evaluation.

3.5.2 In vivo B_1 inhomogeneities

In reality, within the brain and cord, B_1 inhomogeneities do not reach ±50%.

To figure out a realistic range of B_1 inhomogeneities, measurements were done on a cohort of 30 subjects, including 15 HC (15 men; age, 48.7 ± 9.5 years; range, 37 - 71 years) and 15 rugby players (15 men; age, 46.9 ± 7.7 years; range, 34 - 62 years). using an additional sequence (turbo-flash with and without preparation, allowing to reconstruct a map of B_1 inhomogeneities [24][26]. B_1 inhomogeneity (or radiofrequency inhomogeneity) depends on both coil design and body composition. For a given coil (here spine coil), the rugby players represented the worst case of inhomogeneities in the SC because of their body structure, and especially their large neck (spine located in an area where the coil design is less efficient).

C_level	HC+Rugby	HC	Rugby
1	[14.7 % ; 23.0 %] (18.5 ± 2.0) %	[14.7 % ; 21.9 %] (17.6 ± 1.7) %	[16.7 % ; 23.0 %] (19.3 ± 1.9) %
2	[12.7 % ; 19.6 %] (15.5 ± 1.8) %	[12.7 % ; 19.6 %] (15.0 ± 1.6) %	[12.7 % ; 18.9 %] (16.0 ± 1.9) %
3	[6.9 % ; 16.6 %] (11.8 ± 2.0) %	[9.4 % ; 16.6 %] (12.1 ± 1.7) %	[6.9 % ; 15.2 %] (11.5 ± 2.2) %
4	[-0.9 % ; 11.7 %] (6.41 ± 2.7) %	[4.7 % ; 11.7 %] (7.7 ± 1.9) %	[-0.9 % ; 10.7 %] (5.1 ± 2.9) %
5	[-9.7 % ; 6.0 %] (-0.0 ± 3.8) %	[0.0 % ; 6.0 %] (2.5 ± 1.9) %	[-9.7 % ; 5.4 %] (-2.5 ± 3.6) %
6	[-17.6 % ; 0.5 %] (-6.3 ± 4.5) %	[-5.9 % ; 0.5 %] (-3.0 ± 2.0) %	[-17.6 % ; -0.8 %] (-9.5 ± 4.0) %
7	[-25.6 % ; 5.2 %] (-13.2 ± 5.0) %	[-12.3 % ; -5.2 %] (-9.6 ± 2.2) %	[-25.6 % ; -7 %] (16.7 ± 4.5) %

Table 3: Inhomegeneities on the 30 subjects included in this study, per vertebral level, from C1 to C7

In the spinal cord, ΔB_1 values ranged between [-25.6 % - 23.0 %]. Thus regarding the table of T_1 relative error (figure 14.b), such inhomogeneities can lead to a relative error close to 10% in T_1 calculation, which would bias the T_1 evaluation. Such errors exceed the T_1 reproducibility (1 or 2 %) and standard error within a ROI, they should thus be corrected to be fully exploited in a clinical context, where sensitive and robust biomarkers are required

Conclusion

Finally, the tools I used, especially the Z-score, can provide some information that could help for the prognosis or to establish the severity of the impairment, but at the current stage, it is not sufficient enough. It would require further investigation as well as more inclusion to improve its statistical power in order to guide clinical decisions and become trustworthy.

Overall, I draw a very positive conclusion from this internship which was really rewarding on both professional and personal aspects. On the one hand, I had the opportunity to discover the research field, which I was really interested in. Even if I did not have to lead a complete project, the various missions I completed helped me to understand various facets of this domain. On the other hand, on the personal level, this internship has consolidated my choice toward the medical field and clarified some aspects on the career I would like to have, especially orienting myself in the research area.

References

[1] Anatomie du cerveau et du système nerveux - Fédération pour la recherche sur le cerveau (FRC). (2021, 3 février). Fédération pour la Recherche sur le Cerveau (FRC). https://www.frcneurodon.org/comprendre-le-cerveau/a-la-decouverte-du-cerveau/anatomie-du-cerveau-et-du-systeme-nerveux/

[2] Natali AL, Reddy V, Bordoni B. Neuroanatomy, Corticospinal Cord Tract. [Updated 2022 Aug 22]. In: StatPearls [Internet]. Treasure Island (FL): StatPearls Publishing; 2023 Jan-. Available from: https://www.ncbi.nlm.nih.gov/books/NBK535423/

[3] Diaz, E., & Morales, H. (2016). Spinal cord anatomy and clinical syndromes. Seminars in Ultrasound Ct and Mri, 37(5), 360-371. https://doi.org/10.1053/j.sult.2016.05.002

[4] Introduction on NMR principle (Chapter I : Physical principles of NMR Nuclear Magnetism, Resonance, Relaxation) Thomas Christen (2023)

[5] Introduction on MRI Principles (Chapter I, II, III), Thomas Christen (2023)

[6] The challenges of MRI, ISTE Encyclopédie Science – Département Ingénierie et Système – Domaine Image, ISTE Science Publishing LTD (London, UK), 2023.

[7] De Leener B, Fonov VS, Collins DL, Callot V, Stikov N, Cohen-Adad J. PAM50: Unbiased multimodal template of the brainstem and spinal cord aligned with the ICBM152 space. Neuroimage. 2018 Jan 15;165:170-179. doi: 10.1016/j.neuroimage.2017.10.041. Epub 2017 Oct 21. PMID: 29061527.

[8] De Leener B, Levy S, Dupont SM, Fonov VS, Stikov N, Louis Collins D, Callot V, Cohen-Adad J. SCT: Spinal Cord Toolbox, an open-source software for processing spinal cord MRI data. Neuroimage 2017

[9] Lévy S, Benhamou M, Naaman C, Rainville P, Callot V, Cohen-Adad J. White matter atlas of the human spinal cord with estimation of partial volume effect. Neuroimage. 2015 Oct 1;119:262-71. doi: 10.1016/j.neuroimage.2015.06.040. Epub 2015 Jun 19. PMID: 26099457.

[10] Marques JP, Kober T, Krueger G, van der Zwaag W, Van de Moortele PF, Gruetter R. MP2RAGE, a self bias-field corrected sequence for improved segmentation and T_1-mapping at high field. Neuroimage. 2010 Jan 15;49(2):1271-81. doi: 10.1016/j.neuroimage.2009.10.002. Epub 2009 Oct 9. PMID: 19819338.

[11] Rasoanandrianina H, Grapperon AM, Taso M, Girard OM, Duhamel G, Guye M, Ranjeva JP, Attarian S, Verschueren A, Callot V. Region-specific impairment of the cervical spinal cord (SC) in amyotrophic lateral sclerosis: A preliminary study using SC templates and quantitative MRI (diffusion tensor imaging/inhomogeneous magnetization transfer). NMR Biomed. 2017 Dec;30(12). doi: 10.1002/nbm.3801. Epub 2017 Sep 19. PMID: 28926131.

[12] S. Demortière, P. Lehmann, J. Pelletier, B. Audoin, V. Callot. Improved Cervical Cord Lesion Detection with 3D-MP2RAGE Sequence in Patients with Multiple Sclerosis. American Journal of Neuroradiology May 2020

[13] Massire A, Rasoanandrianina H, Guye M, Callot V. Anterior fissure, central canal, posterior septum and more: New insights into the cervical spinal cord gray and white matter regional organization using T_1 mapping at 7T. Neuroimage. 2020 Jan 15;205:116275. doi: 10.1016/j.neuroimage.2019.116275. Epub 2019 Oct 13. PMID: 31618700.

[14] Samira Mchinda, Arnaud Le Troter, Sarah Demortière, Nilser Laines Medina, Lauriane PINI, Jean Pelletier, Bertrand Audoin and Virginie Callot. Z-score maps to characterize spinal cord lesions in MS patients: Toward a semi-automated lesion identification/segmentation method

[15] Jenkinson M, Beckmann CF, Behrens TE, Woolrich MW, Smith SM. FSL. Neuroimage. 2012 Aug 15;62(2):782-90. doi: 10.1016/j.neuroimage.2011.09.015. Epub 2011 Sep 16. PMID: 21979382.

[16] Chen, J. (2022). Z-Test Definition : Its uses in statistics simply explained with example. Investopedia.

[17] Arash Forodighasemabadi, Lucas Soustelle, Olivier M. Girard, Thomas Troalen, Jean-Philippe Ranjeva, Guillaume Duhamel and Virginie Callot. Brain and cervical spinal cord myelination and age-related changes in adulthood: a preliminary study based on ihMTsat and T_1 relaxometry mapping

[18] Sclérose latérale amyotrophique (SLA) / Maladie de charcot · InserM, La science pour la santé. (s. d.). Inserm.

[19] Cedarbaum JM, Stambler N, Malta E, Fuller C, Hilt D, Thurmond B, Nakanishi A. The ALSFRS-R: a revised ALS functional rating scale that incorporates assessments of respiratory function. BDNF ALS Study Group (Phase III). J Neurol Sci. 1999 Oct 31;169(1-2):13-21. doi: 10.1016/s0022-510x(99)00210-5. PMID: 10540002.

[20] Tsushima E. Interpreting Results from Statistical Hypothesis Testing: Understanding the Appropriate P-value. Phys Ther Res. 2022;25(2):49-55. doi: 10.1298/ptr.R0019. Epub 2022 May 13. PMID: 36118788; PMCID: PMC9437930.

[21] Milligan J, Ryan K, Fehlings M, Bauman C. Myélopathie cervicale dégénérative: Diagnostic et prise en charge en première ligne. Can Fam Physician. 2019 Sep;65(9):e379-e385. French. PMID: 31515323; PMCID: PMC6741798.

[22] Gembruch O, Jabbarli R, Rashidi A, Chihi M, El Hindy N, Wetter A, Hütter BO, Sure U, Dammann P, Özkan N. Degenerative Cervical Myelopathy in Higher-Aged Patients: How Do They Benefit from Surgery? J Clin Med. 2019 Dec 26;9(1):62. doi: 10.3390/jcm9010062. PMID: 31888031; PMCID: PMC7019793.

[23] Tetreault L, Kopjar B, Nouri A, Arnold P, Barbagallo G, Bartels R, Qiang Z, Singh A, Zileli M, Vaccaro A, Fehlings MG. The modified Japanese Orthopaedic Association scale: establishing criteria for mild, moderate and severe impairment in patients with degenerative cervical myelopathy. Eur Spine J. 2017 Jan;26(1):78-84. doi: 10.1007/s00586-016-4660-8. Epub 2016 Jun 24. PMID: 27342612.

[24] Massire A, Taso M, Besson P, Guye M, Ranjeva JP, Callot V. High-resolution multi-parametric quantitative magnetic resonance imaging of the human cervical spinal cord at 7T. Neuroimage. 2016 Dec;143:58-69. doi: 10.1016/j.neuroimage.2016.08.055. Epub 2016 Aug 26. PMID: 27574985.

[25] Forodighasemabadi A, Rasoanandrianina H, El Mendili MM, Guye M, Callot V. An optimized MP2RAGE sequence for studying both brain and cervical spinal cord in a single acquisition at 3T. Magn Reson Imaging. 2021 Dec;84:18-26. doi: 10.1016/j.mri.2021.08.011. Epub 2021 Sep 10. PMID: 34517015.

[26] Rasoanandrianina H, Massire A, Taso M, Guye M, Ranjeva JP, Kober T, Callot V. Regional T_1 mapping of the whole cervical spinal cord using an optimized MP2RAGE sequence. NMR Biomed. 2019 Nov;32(11):e4142. doi: 10.1002/nbm.4142. Epub 2019 Aug 8. PMID: 31393649.

Summary

Spinal cord impairments can lead to varying degrees of motor, sensory, and autonomic dysfunction, often resulting in paralysis or loss of sensation. Magnetic Resonance Imaging can help to assess the diagnosis, but conventional techniques are usually insufficient to characterize underlying impairments and assess a prognosis. This is why quantitative MR techniques are needed, to help detection at an early stage and provide objective measurements that could be used for longitudinal follow-up. In addition to diagnosis by specialists, automatic postprocessing tools are developed in order to identify and even segment lesions or impairments in a spinal cord MRI. The one investigated in this paper is the Z-score, a statistical scoring able to detect outliers from a dataset. Thus, considering a set of MRI acquired on healthy controls, the Z-score should be able to identify a pathological subject, and the regions of impairment. In the end, this technique has been tested for patients suffering from two pathologies, and even if some lesions have been detected, this tool is not yet convincing enough to guide clinical decisions on its own.

Résumé

Les détériorations de la moelle épinière peuvent causer plusieurs degrés de handicaps moteurs ou sensoriels, menant souvent à une paralysie ou une perte de sensibilité. L'Imagerie par Résonance Magnétique peut aider à l'établissement d'un diagnostic, mais les techniques conventionnelles ne permettent souvent pas à caractériser les déficiences sous-jacentes et délivrer un pronostic. C'est pourquoi des techniques quantitatives d'IRM sont nécessaires pour faciliter la détection à un stade précoce et fournir des mesures objectives qui pourraient être utilisées pour le suivi. De plus, certains outils sont développés pour identifier automatiquement, voire même segmenter des lésions sur un IRM médullaire. L'outil étudié dans ce rapport est le Z-score, une statistique permettant de détecter une valeur aberrante au sein d'une liste de données. Ainsi, en considérant plusieurs IRM acquis sur des sujets sains, le Z-score devrait être capable d'identifier un sujet pathologique ainsi que les régions lésionnées. Finalement, cette technique a été testée sur des patients souffrants de deux pathologies distinctes, et même si certaines lésions ont été détectées, cet outil n'est pas encore assez convaincant pour guider des décisions cliniques de lui-même.